TISSUE ENGINEERING: Part A
Volume 00, Number 00, 2020

DOI: 10.1089/ten.tea.2020.0194

termis
Tissue Engineering
& Regenerative Medicine
International Society

Comparison Study of Stem Cell-Derived Extracellular Vesicles for Enhanced Osteogenic Differentiation

Elham Pishavar, BS,[1,2,*] Joshua S. Copus, BS,[1,3,*] Anthony Atala, MD,[1,3] and Sang Jin Lee, PhD[1,3]

Stem cell-derived extracellular vesicles (EVs) have shown great promise in the field of regenerative medicine and tissue engineering. Recently, human bone marrow-derived mesenchymal stem cell (BMSC)-derived EVs have been considered for bone tissue engineering applications. In this study, we evaluated the osteogenic capability of placental stem cell (PSC)-derived EVs and compared them to the well-characterized BMSC-derived EVs. EVs were extracted from three designated time points (0, 7, and 21 days) after osteogenic differentiation. The results showed that the PSC-derived EVs had much higher protein and lipid concentrations than EVs derived from BMSCs. The extracted EVs were characterized by observing their morphology and size distribution before utilizing next-generation sequencing to determine their microRNA (miRNA) profiles. A total of 306 miRNAs within the EVs were identified, of which 64 were significantly expressed in PSC-derived EVs that related to osteogenic differentiation. *In vitro* osteogenic differentiation study indicated the late-stage (21-day extracted)-derived EVs higher osteogenic enhancing capability when compared with the early stage-derived EVs. We demonstrated that EVs derived from PSCs could be a new source of EVs for bone tissue engineering applications.

Keywords: extracellular vesicles, miRNAs, mesenchymal stem cells, placental stem cells, osteogenic differentiation, tissue engineering

Impact Statement

Bone tissue engineering approaches aim to overcome current challenges associated with autologous bone grafts by delivering a combination of scaffolding material, cells, and bioactive factors to enhance bone regeneration. Extracellular vesicles (EVs) from bone marrow-derived mesenchymal stem cells (BMSCs) have recently been shown to enhance osteogenic differentiation and improve bone mineral deposition. Herein, EVs derived from placental stem cells (PSCs) have a comparative ability to improve osteogenic capability. PSCs have advantages such as higher proliferation capacity, the ability to be harvested without an invasive procedure, and they produce larger amounts of EVs. The feasibility of using these EVs will be especially important in clinical translational studies, which require substantial amounts of EVs to achieve this effect.

Introduction

In the United States alone, each year over 500,000 bone grafts are used to treat bone defects or disorders. The bone grafting products and procedures result in a burden of over $2.5 billion to the health care system, which is expected to double by 2020.[1] Currently, autologous bone grafts are considered the gold standard for reconstructive surgery, but they are still limited as they require a second operation to harvest the bone tissue, which can often result in donor-site morbidity.[2] To avoid this, bone tissue engineering is an alternative option that combines scaffolds, cells, and bioactive factors to enhance bone regeneration.[3,4]

The use of bone marrow-derived mesenchymal stem cells (BMSCs) has been a common approach for bone tissue engineering applications.[5] To improve the efficacy of stem cells used for bone tissue engineering, bioactive molecules (e.g., growth factors and cytokines) are commonly incorporated

[1]Wake Forest Institute for Regenerative Medicine, Wake Forest School of Medicine, Winston-Salem, North Carolina, USA.
[2]Pharmaceutical Research Center, Pharmaceutical Technology Institute, Mashhad University of Medical Sciences, Mashhad, Iran.
[3]School of Biomedical Engineering and Sciences, Wake Forest University-Virginia Tech, Winston-Salem, North Carolina, USA.
*These two authors contributed equally to this work.

with cells into a scaffolding material. Typically, growth factors such as bone morphogenetic proteins (BMPs), vascular endothelial growth factors, and insulin-like growth factors have been used for bone tissue engineering. Especially, BMPs are a family of osteogenic growth factors that include BMP-2 and BMP-7, which have both been incorporated onto FDA-approved devices.[6] However, growth factors for bone regeneration have been limited due to their rapid degradation in physiological conditions as well as their deactivation by enzymes.[6] A variety of both organic and inorganic nanoparticles have been utilized to overcome these challenges.[7]

Most nanoparticles used for bone tissue engineering have attempted to deliver bioactive molecules, such as BMP-2.[8,9] or dexamethasone[10] to directly control differentiation fate of native stem cells or to improve bone mineral deposition, but these osteogenic molecules are still limited in their effectiveness due to their short *in vivo* half-life, the low loading efficiencies associated with nanoparticles,[11] their toxicity, and the large quantities of nanoparticles needed for therapeutic effect.[6]

MicroRNAs (miRNAs) are small, noncoding RNAs that influence cell proliferation, differentiation, and apoptosis by degrading or inhibiting the translation of mRNAs.[12] Unlike other bioactive molecules, miRNAs have the target-specific nature that modulates specific genes.[13] Thus, researchers have recently been interested in delivering miRNAs associated with osteogenesis to improve osteogenic differentiation of BMSCs and therefore bone tissue regeneration.[14–16]

Although bone-specific miRNAs play a vital role in bone remodeling,[17] their use has been limited due to the difficulty with delivering them to target cells without interference from degrading enzymes. Some research groups have developed lipid-based,[18] and even polymeric nanoparticles[19] to deliver miRNAs. Single miRNA delivery still lacks the therapeutic potential of delivering multiple miRNAs especially in bone remodeling, where the miRNAs involved act to both inhibit osteoclast activity[20] as well as increasing osteoblast activity.[21] This results in a net increase in the bone mineral deposition that is much greater than the effect of delivering either miRNA alone.

To overcome these limitations, researchers have recently found that naturally derived extracellular vesicles (EVs) can be used as vesicles to deliver multiple miRNAs to target cells. EVs include exosomes, which are small nanovesicles composed of lipid membranes and are excreted by all cell types. These nanovesicles are involved in cell communication, protein transfer, and delivery of miRNAs to surrounding cells.[22] They can be easily extracted from bodily fluids or cell culture medium[22] and also have advantages such as low immunogenicity, high stability, and an intrinsic homing effect, which makes them easily absorbed by target cells,[23,24] where the osteogenic miRNAs can then be delivered.

BMSC-derived EVs have been shown to play a key role in the maintenance of bone remodeling.[25] These EVs offered the enhanced osteogenic differentiation of BMSCs and improved bone formation depending on their miRNA profile. The miRNA profile of a stem cell-derived EV depends on the cell source[26,27] and stage/time point of differentiation. Moreover, the use of BMSCs is limited as they are not readily abundant and require an invasive procedure to be harvested from the donor. The BMSCs are also limited in their passage capabilities, where a typical BMSC will lose its stemness around passage 10.[28]

Placental stem cells (PSCs) have a faster proliferation rate[28,29] and can be expanded to larger passage numbers while still maintaining their stemness. PSCs have been shown to have a proliferation capacity of around 30 passages, which is almost triple the capacity of adult BMSCs.[28] This is due to the PSCs being closer to embryonic tissue than BMSCs that are typically harvested from adult tissue, which gives them limited differentiation capabilities.[28] PSCs can also be easily harvested for autogenic or allogeneic use from the postpartum placental tissue without the need for any invasive procedures associated with BMSCs.[30] Taken together, this indicates that PSCs may be a good candidate to isolate large quantities of EVs. PSCs have also been shown to exhibit osteogenic differentiation capabilities[31] and have been widely used in tissue engineering applications due to their differentiation capabilities and immunomodulation properties.[32] Although EVs from BMSCs are well characterized, the effect of osteogenic differentiation on PSC-derived EV content is poorly understood.

In this study, we aimed to compare the ability of PSC-derived EVs to differentiate with the well-characterized BMSC-derived EVs (Fig. 1). We further aimed to prove the feasibility of utilizing these EVs for bone tissue engineering applications. Since

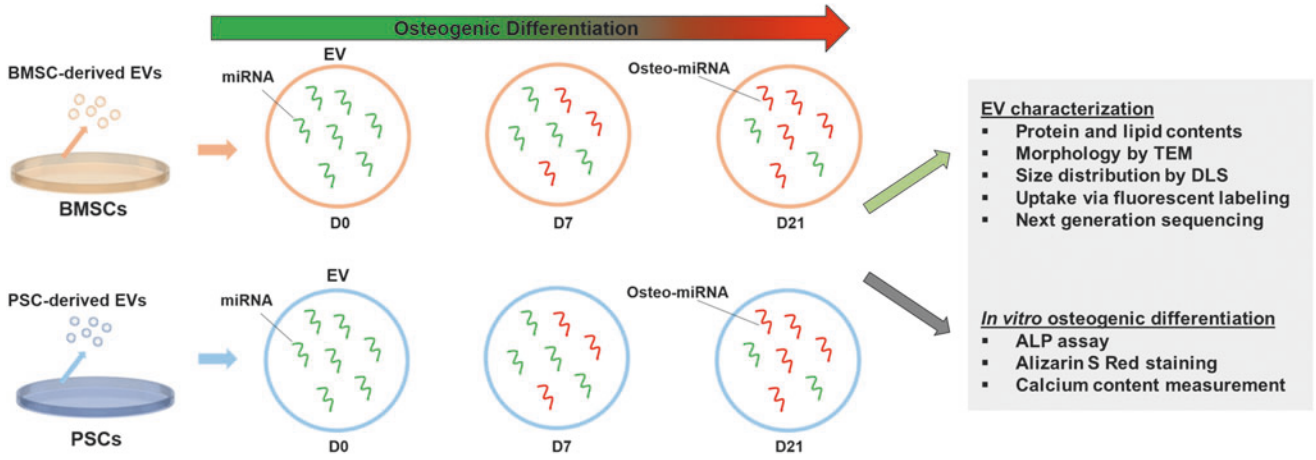

FIG. 1. Schematic diagram of the experimental design for comparison study. Color images are available online.

PSCs exhibit the ability to differentiate into osteogenic cell lines, we hypothesized that EVs isolated from these cells during differentiation could enhance the osteogenic differentiation of BMSCs. We evaluated the effects of cell source and stage of differentiation on the miRNA content of EVs.

Materials and Methods

Cell culture and EV isolation

Human BMSCs (ATCC, Manassas, VA) were purchased and expanded to passage 3 to 5 before being cultured in EV-free media prepared according to Wang *et al.*[33] Human PSCs were obtained and isolated from healthy donors with informed consent approved according to the procedures of the Institutional Review Board (IRB) at Wake Forest University (Winston-Salem, NC), and cells from passage 11 were cultured in EV-free media.[33] Briefly, both BMSCs and PSCs were expanded in growth medium containing Dulbecco's modified Eagle's medium (DMEM; Gibco, Thermo Fisher Scientific, Waltham, MA), 10% (v/v) fetal bovine serum (ScienCell, Carlsbad, CA), 100 U/mL penicillin G, and 100 mg/mL streptomycin (Gibco, Thermo Fisher Scientific) at 37°C in an incubator with 5% CO_2 atmosphere and 100% relative humidity. To induce osteogenic differentiation, BMSCs and PSCs were cultured in an osteogenic medium (OM), including 10 nM dexamethasone, 100 μM ascorbic acid, and 2 mM β-glycerophosphate on T175 tissue culture flasks for 21 days. Fresh culture medium was replaced every third day. All chemical reagents were obtained from Millipore Sigma (St. Louis, MO) unless stated otherwise.

For EV isolation, multiple batches of BMSCs and PSCs were utilized for isolation, and the isolation was repeated on multiple passages as well. Briefly, the culture medium was replaced with a serum-free culture medium for 72 h. The medium was then collected, and EVs were isolated by a series of differential centrifugation with filtration. Briefly, the supernatant was centrifuged at 1000 *g* for 30 min at 4°C to eliminate larger cellular particles. This was then concentrated and filtered through the KR2i TFF system (Spectrum Labs, High Point, NC) using the concentration–diafiltration–concentration mode. On average, the supernatant collected was between 200 and 500 mL and was usually run through the system until it reached a volume of 250 mL. This was the concentration step, which was then followed by diafiltration with 500–100 mL phosphate-buffered saline (PBS), which was then concentrated to 10 mL. The system utilized 500 kDa modified polyethersulfone filter tubes and proceeded at a flow rate of 80 mL/min and a pressure limit of 8 psi for the filter module D02-E500-05-N. This procedure has been previously established by Yoo *et al.*[34] After that, supernatant was centrifuged at 500 *g* for 20 min at 4°C, followed by passing through a 0.22 μm filter to eliminate debris. Then, the supernatant was ultracentrifuged at 120,000 *g* for 70 min in a T-647.5 rotor (Sorvall WX Ultra series; Thermo Scientific). The EV pellets were gently suspended in PBS and frozen at −80°C since it has been previously established that these are optimal long-term storage conditions.[35]

Quantifying EV concentration

The EV yield was quantified by two different measures as is standard according to the MISEV2018 guidelines. First, the total protein concentration was measured using the BCA Protein Assay Kit (Thermo Fisher Scientific). Next, total lipid concentration was quantified using the Lipid Quantification Kit (STA-613; Cell Biolabs, San Diego, CA) previously used by other groups investigating EVs.[36] Briefly, 15 μL of each EV group was added to a 96-well plate and incubated uncovered for 30 min at 90°C. The samples were then transferred to 4°C for 5 min before adding 150 μL of 18 M sulfuric acid. They were then incubated at 90°C for 10 min and again transferred to 4°C for 5 min. Next, 100 μL of each sample was transferred to a clean 96-well plate before being read at 540 nm to determine the background. One hundred microliters of Vanillin Reagent was then carefully mixed and incubated at 37°C for 15 min before reading at 540 nm to determine the signal. The background was subtracted from the signal and compared with a previously prepared standard curve.

EV characterization

The EV morphology was observed by transmission electron microscopy (TEM). For TEM, EVs were fixed with 2% paraformaldehyde for 15 min before imaging. Approximately 8 μL of the EV solution was deposited onto a carbon-coated copper grid and allowed to dry at room temperature for 10 min before staining with 1% uranyl acetate twice (6 min each). A FEI Tecnai BioTwin TEM (Thermo Fisher Scientific) was used to image the EVs. To determine the size distribution, dynamic light scattering (DLS; Brookhaven Instruments Corporation; Holtsville, NY) was utilized for early (0 day; D0), middle (7 days; D7), and late (21 days; D21) time points of osteogenic differentiation.

EV uptake

To examine whether the BMSCs internalize EVs, the BMSCs were seeded at 20,000 cells/cm^2 on chamber slides (Millipore, Billerica, MA) and allowed to attach for 12 h. All six EV groups were labeled with a PKH67 Green Fluorescent Cell Linker Kit. PKH67-labeled EVs were diluted in the culture medium and then delivered to the BMSCs in the culture at a concentration of 10 μg/mL medium based on reported therapeutic doses of EVs.[33] After 48 h, the cells were washed with PBS to remove noninternalized EVs, and then fixed with 2% formaldehyde for 15 min, and washed again. BMSCs were then stained with 4′,6-diamidino-2-phenylindole (DAPI; Thermo Fisher Scientific), which is blue fluorescent nuclei stain. The chamber slides were then mounted with VECTASHIELD HardSet Mounting Medium (Vector Laboratories, Burlingame, CA) and visualized using confocal microscopy (Leica TCS LSI Macro Confocal).

miRNA profiling of EVs

The total miRNA of each EV group was extracted using the miRCURY™ RNA Isolation Kit (Qiagen, Venlo, Netherlands), according to the manufacturer's protocol. Total RNA, including the miRNA fraction, was used as the starting material to prepare cDNA libraries using the CleanTag™ Library Kit from TriLink Biotechnologies (Cat No. L-3206). In brief, adapters are ligated to the 5′ phosphate and 3′ hydroxyl groups, reverse transcribed, polymerase chain reaction amplified, and then purified using AMPure® XP Beads. Each cDNA Library was validated and

checked for size distribution using the High-Sensitivity DNA Kit on the Agilent 2100 Bioanalyzer. The quantity of each library was measured using the Qubit 3.0 (Thermo Fisher) and loaded on the Illumina Mid Output 150 Cycle Kit and sequenced using the Illumina NextSeq 500.

Differentially expressed miRNAs were analyzed between early (D0) and late (D21) osteogenic culture time, as well as between EV cell sources of PSC and BMSCs. Once the miRNAs were identified, the target gene and pathways could be predicted utilizing two previously established and open-source algorithms: DIANA-microT-CDS and DIANA-TarBase v7.0.[37,38] Following the protocols previously established, the microT threshold was set at a score of 0.8 when utilizing the DIANA-microT-CDS algorithm for target gene prediction. DIANA-mirPath v.3[38] was used for clustering analysis of the miRNAs, as well as determining the known KEGG pathways.[39] The algorithm uses experimentally validated interactions to predict miRNA targets.[40,41] The algorithm then creates a graphical summary of the predicted targets and pathways that may be affected by the identified miRNAs based off of previously experimentally validated results.[42] The program also automatically calculates statistical significance, which was manually set at a value of 0.05, by utilizing Benjamini and Hochberg's false discovery rate (FDR). The FDR is a statistical method for controlling incorrect rejections of the null hypothesis when conducting multiple comparisons, which is common during miRNA analysis. This is in accordance with Wang *et al.*[43] who reported miRNA pathways utilizing the same software systems.

EV-stimulated osteogenic differentiation of BMSCs

BMSCs (passage 3) were seeded at a density of 18,000 cells/cm^2 in 24-well plates in EV-free OM. After overnight attachment, the culture medium was replaced by media containing EVs. In total, six different EV groups were tested. Both PSC and BMSC EVs isolated at different osteogenic differentiation time points (D0, D7, and D21) were used. The BMSCs were continuously treated with the previously reported therapeutic dosage of 10 μg/mL EVs for all *in vitro* experiments,[33] and media were changed every 3 days.

Alkaline phosphatase assay

After 7 and 14 days of treatment, BMSCs were rinsed with DMEM and lysed using Triton X-100 (One-Step Kit; Thermo Fisher Scientific). The alkaline phosphatase (ALP) activity was measured using *p*-nitrophenyl phosphate as the substrate. The quantity of *p*-nitrophenol produced by the cells directly corresponds to the ALP activity according to the protocol.

Alizarin red S staining assay

To characterize the mineralization of BMSCs after EV treatment an Alizarin Red assay was conducted. Cells were cultured for 7, 10, 14, and 21 days with EV treatment before being washed and fixed following the protocol as mentioned above. After fixation, the cells were washed with distilled water and incubated with Alizarin Red solution for 5 min. The extra dye was removed by rinsing with distilled water three times. Images were collected through light microscopy (Leica DM4000 B). To quantify calcium deposition, 200 μL of 10% acetic acid was added to each Alizarin Red stained well and shaken for 30 min. The cells were then collected and transferred into a microcentrifuge tube, where they were vortexed for 30 s. They were then heated to 85°C for 10 min before being cooled on ice for 5 min. The slurry was centrifuged for 15 min and the supernatant moved to another tube where it was neutralized with 10% ammonium hydroxide. This was then added to a 96-well plate and the absorbance was read on a plate reader (SpectraMax M5 Microplate Reader). The concentration was compared with a standard curve for quantification. The Alizarin Red staining assay was performed at 7, 10, 14, and 21 days.

Statistical analysis

Data are reported three times as the mean ± standard deviation. The data were analyzed statistically employing a one-way analysis of variance (ANOVA) using GraphPad PRISM® 8.0 software and p-values <0.05 indicate statistically significant differences. The miRNA sequencing raw data were normalized based on the DESEQ normalized expression data. KEGG molecular pathway enrichment was reported where FDR was <0.001.

Results

Characterization of stem cell-derived EVs

EVs were isolated from both BMSCs and PSCs cultured in growth media (D0) as well as osteogenic media at 7 days (D7) and 21 days (D21) of culture. The yield of the BMSC-derived EVs was 71.0 ± 38.3, 149.3 ± 22.9, and 123.6 ± 16.9 μg/mL for D0, D7, and D21, respectively. BMSCs exhibited similar yields to the values reported in the literature,[44] but PSCs consistently yielded higher EV protein quantities in comparison to BMSCs. The PSC-derived EVs had yields of 394.6 ± 38.2, 959.3 ± 59.7, and 695.7 ± 90.8 μg/mL at D0, D7, and D21, respectively (Fig. 2A).

The lipid concentration of the EVs was also quantified so that a comparison could be made between the protein to lipid ratios of each EV group as is standard according to International Society for Extracellular Vesicles (ISEV) to ensure EVs are pure and the isolation method does not coisolate unbound proteins. The BMSC-derived EVs had lipid concentrations of 185.2 ± 17.2, 495.2 ± 32.9, and 1339.37 ± 74.2 μg/mL at D0, D7, and D21, respectively. The PSC-derived EVs had lipid concentrations of 3486.5 ± 227.1, 818.1 ± 85.8, and 247.7 ± 8.2 μg/mL at D0, D7, and D21, respectively (Fig. 2B). This means that for the protein to lipid ratios, BMSC-derived EVs had a ratio of 0.383, 0.302, and 0.092 at D0, D7, and D21, respectively, whereas the PSC-derived EVs were 0.113, 1.172, and 2.808 at D0, D7, and D21, respectively.

EVs were characterized by TEM and DLS to confirm that the morphology and size were consistent with the values and shape reported by other groups isolating EVs. The TEM images showed that all six groups of examined EVs had a typical cup-shaped morphology with various hydrodynamic diameters (Fig. 2C). The TEM images revealed that the different groups of isolated EVs featured similar shape and size ranges, confirming that the techniques for isolation yielded consistent batches of EVs.

DLS was also performed to quantitatively confirm the EV size distribution. DLS calculated the hydrodynamic diameter of EVs from the Stokes–Einstein Equation, which is used to characterize how large particles move slower due to Brownian

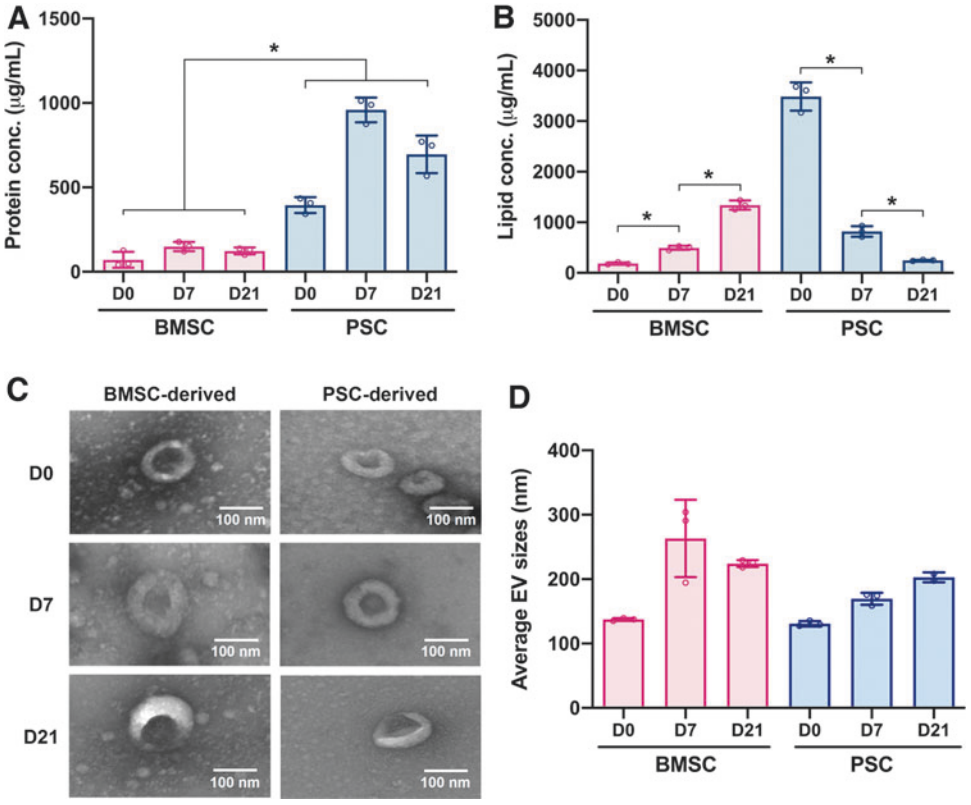

FIG. 2. Characterization of stem cell-derived EVs. **(A)** Protein concentrations. **(B)** Lipid concentrations. **(C)** Morphological analysis by TEM of EVs derived from PSCs and BMSCs at D0, D7, and D21. **(D)** Average hydrodynamic diameters of EVs measured by DLS analysis. All data are represented as mean ± SD. * indicates $p < 0.05$. BMSC, bone marrow-derived mesenchymal stem cell; DLS, dynamic light scattering; EV, extracellular vesicle; PSC, placental stem cell; SD, standard deviation; TEM, transmission electron microscopy. Color images are available online.

motion. From this experiment, we found that the BMSC-derived EVs had diameters of 137.4 ± 8.5, 262.8 ± 32.2, and 224.1 ± 43.3 nm on D0, D7, and D21, respectively. The PSC-derived EVs had diameters of 130.8 ± 9.53, 169.5 ± 32.8, and 202.9 ± 50.7 nm on D0, D7, and D21, respectively.

Internalization of EVs by BMSCs

To explore whether EVs could enter the cytoplasm of BMSCs, the six groups of EVs were labeled with green fluorescence dye PKH67 and incubated with BMSCs for 48 h. Fluorescence microscopy analysis showed that the BMSCs were capable of internalizing the EVs of all groups (Fig. 3). The internalized PKH67 fluorescence varied very little between EV groups and across cells within the culture, which suggests that the EVs were homogenously internalized.

miRNA profiles of EVs during expansion and differentiation

Among the variety of molecules that are contained in EVs, miRNAs have attracted the most attention because of their

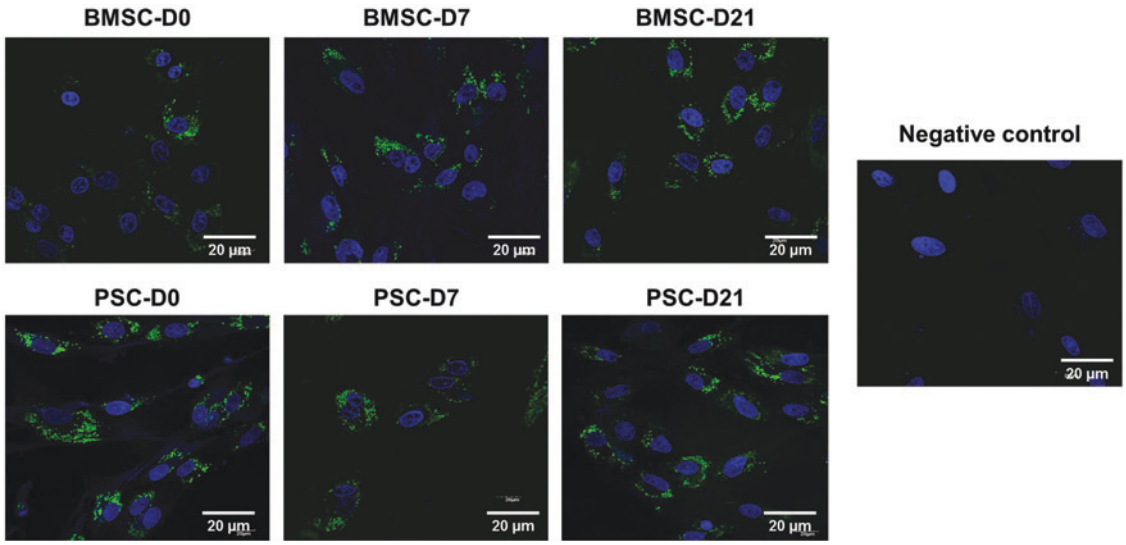

FIG. 3. Visualization of EVs in BMSCs. EVs are labeled in *green* with PKH67, whereas cell nuclei are stained *blue* with DAPI. DAPI, 4′,6-diamidino-2-phenylindole. Color images are available online.

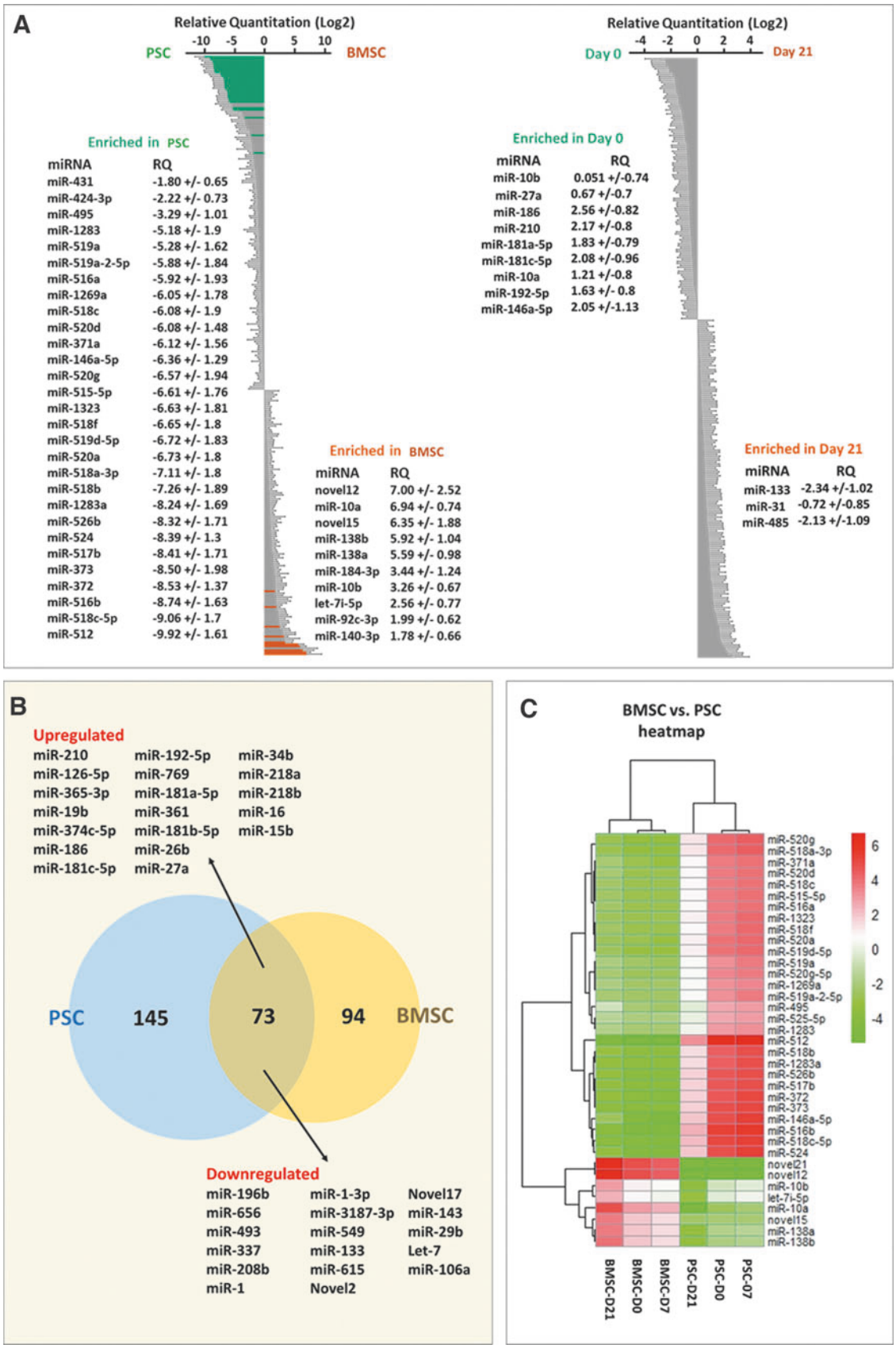

FIG. 4. **(A)** Altered miRNA profiles of EVs derived from two types of stem cells and between D0 and D21. **(B)** Pie chart showing the correlation of the top 44 abundant miRNAs (based on FDR ≤0.05) among EVs derived from both cell types. **(C)** Heatmap of the most abundant miRNAs depiction expression change between cell types and over time. FDR, false discovery rate; miRNA, microRNA. Color images are available online.

regulatory roles in gene expression.[45] For this reason, we determined the content of miRNAs within our EVs. We then moved onto next-generation sequencing to determine the miRNA profiles contained within our EVs. A total of 306 miRNAs were identified in all samples (Supplementary Table S1). Clustering analysis of the miRNA expression in the six groups of EVs revealed marked differences in miRNA expression, and the software system was able to determine biological pathways that were significantly impacted by the identified miRNAs (Fig. 4A and Supplementary Table S2).

Among the differentially expressed miRNAs in D0 versus D21 (Supplementary Table S3), miR-186, miR-210, miR-181c-5p, and miR-146a-5p were increased twofold and miR-133 and miR-485 were decreased twofold in the last stage. Meanwhile, miR-10, miR-27a, and miR-192 increased, which have been reported as late markers of osteogenesis, and miR-31 decreased. In addition, miR-10 and miR-138 were expressed sixfold higher in BMSCs versus PSCs (Fig. 4B, C).

The top 34 KEGG pathways were also reported, which indicated the potential upregulated target genes of the 301 miRNAs that were identified in both BMSC and PSC EVs (Supplementary Fig. S1). Of the potential KEGG pathways analyzed, Wnt signaling was of particular interest due to its role in osteogenic differentiation of MSCs.[46]

EV-stimulated osteogenic differentiation of BMSCs

EVs derived from PSCs and BMSCs during different stages of differentiation were delivered to undifferentiated BMSCs. After 7 and 14 days of treatment, the ALP activity was measured as an early indicator of cell differentiation toward the osteogenic lineage (Fig. 5). Both BMSC-D21 and PSC-D21 EVs significantly increased ALP activity at 7 days of culture in comparison to the positive control in OM. At 14 days, almost all EV groups showed a significant increase in ALP activity, except for BMSC-D0. Alizarin Red S staining (Fig. 6A) and quantification assay (Fig. 6B) demonstrated that calcium deposition significantly increased after 14-day induction by all EVs in comparison to the positive control in OM.

Discussion

The therapeutic potential of BMSC-derived EVs has been well documented.[47–50] Their role in bone remodeling has been investigated both *in vitro* and *in vivo,* and it has been shown that many of the key factors for regulating bone remodeling are targeted by miRNAs contained within the EVs.[51,52] Researchers have focused mainly on utilizing these EVs and their biologically active content to address pathological bone diseases such as osteoporosis, but these EVs also exhibit the potential to improve stem cell differentiation within tissue-engineered bone scaffolds due to their ability to accelerate bone mineral deposition. Most studies utilize EVs derived from BMSCs or mineralizing osteoblasts to achieve this effect, so there exists a lack of knowledge on utilizing alternate cell sources to harvest EVs with the potential to improve bone mineral formation.[53]

In this study, we compared EVs derived from BMSCs and PSCs during the process of osteogenic differentiation in an attempt to better understand the role that cell source and culture conditions have on the therapeutic effect of these EVs. The EVs were delivered in combination with OM, which enhances their osteogenic effect, but they do exhibit the potential for osteogenic differentiation when delivered alone.[23,33] It has been shown that the miRNA profile within EVs changes depending on the stage of differentiation[54]; however, this effect has not been studied while comparing different mesenchymal stem cells. We isolated and characterized EVs derived from BMSCs and PSCs and investigated the differentiation capabilities of EVs secreted under different stages of osteogenic differentiation. Within this study, we aimed to determine the effects of both cell type and differentiation stage, on EV content, and the downstream effect on the regulation of osteogenic differentiation.[54] By doing so, we have proven the feasibility of utilizing alternative cell sources of EVs for future studies involving osteogenic differentiation.

The isolated EV groups did not exhibit any statistically significant differences in size, regardless of cell source. This confirms the consistency of the isolation process utilized for EV separation. When comparing between differentiation time within the same cell source, the isolated EVs exhibited larger size distributions at D21 compared with D0 with

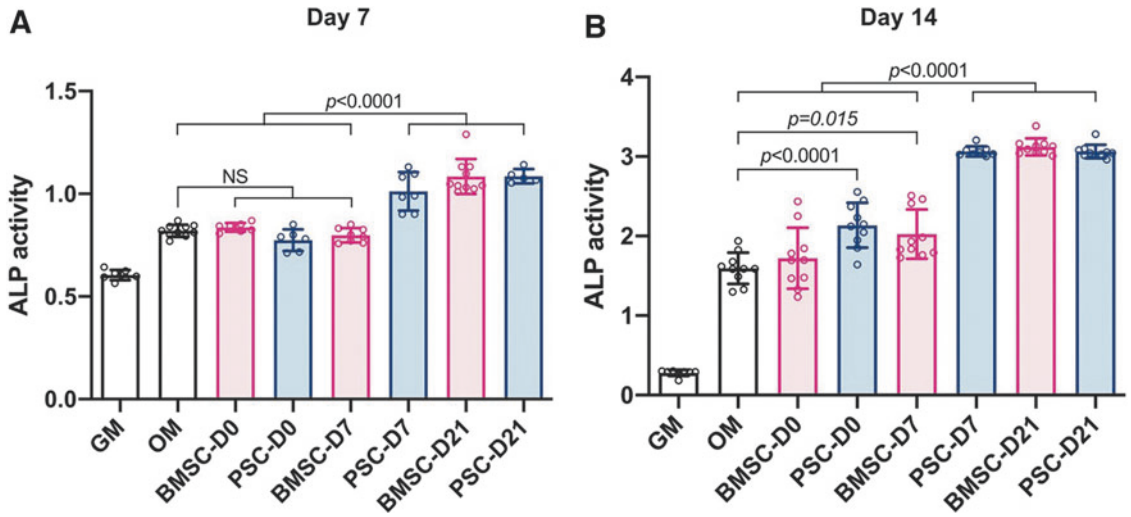

FIG. 5. ALP activity of BMSCs after incubation with EVs (10 μg/mL) after **(A)** 7 and **(B)** 14 days of osteogenic differentiation. All data are represented as mean ± SD. ALP, alkaline phosphatase. Color images are available online.

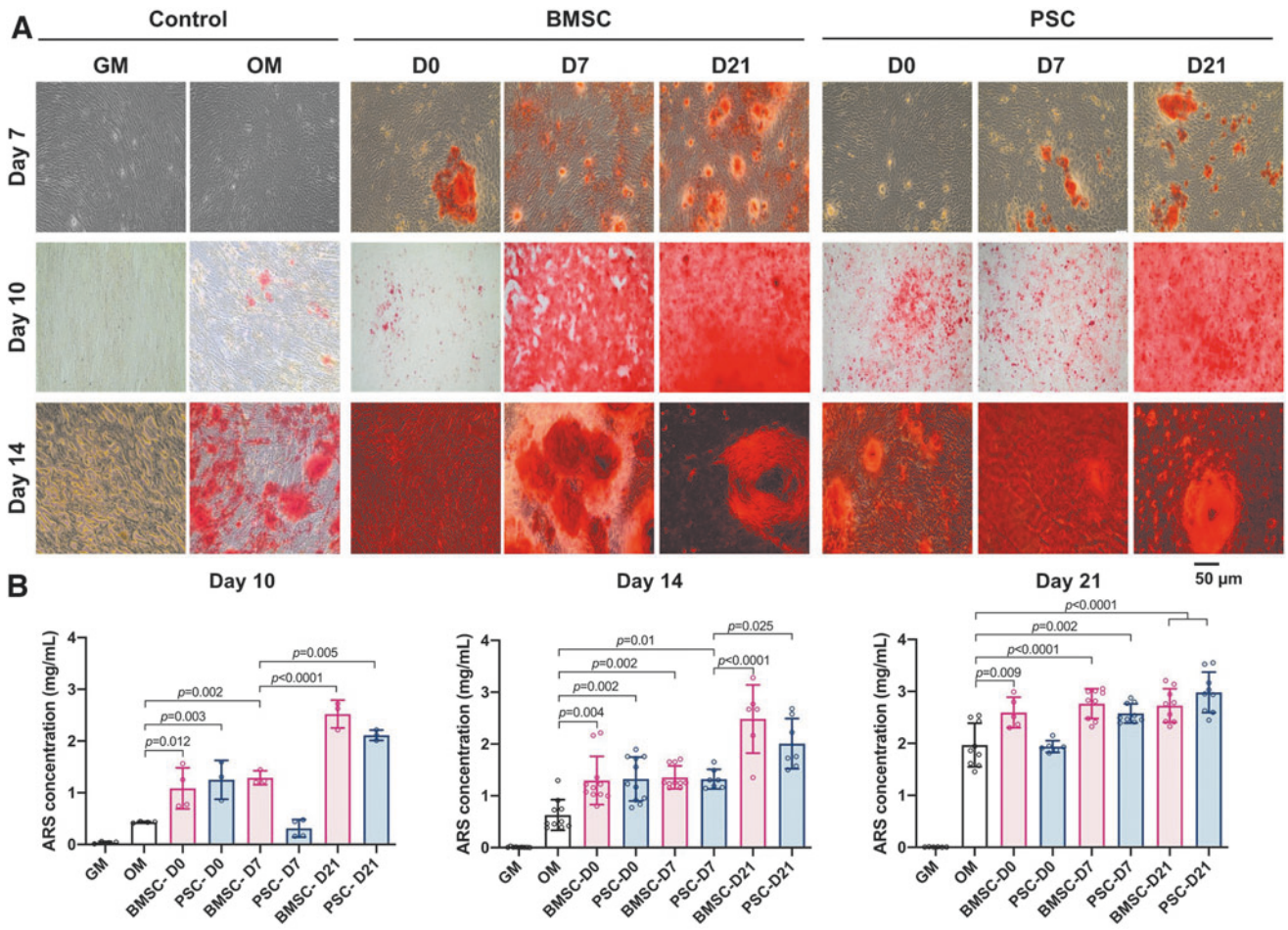

FIG. 6. Calcium content assay: **(A)** Alizarin Red S-stained images at 7, 10, and 14 days after osteogenic differentiation. **(B)** Calcium contents at 10, 14, and 21 days after osteogenic differentiation. All data are represented as mean ± SD. Color images are available online.

$p = 0.004$ for BMSC-derived and $p = 0.0369$ for PSC-derived EVs. This may be due to the larger cell membrane surface area available for EV formation since the cell morphology of MSCs become less spindle like due to the cells differentiating into osteoblast-like cells.[55]

Characterizing the protein concentration between cell groups yielded large differences between cell source with the PSC-derived EVs consistently yielding higher protein concentrations. When analyzing the lipid concentrations of each EV group, we found that the PSC-derived EVs also had significantly higher lipid concentrations at all time points with the exception of D21. The trend of isolating both higher protein concentrations and lipid concentrations from PSCs suggests that there was a larger total yield of EVs from these cells when compared with BMSCs. When comparing the protein to lipid ratio, which is a common quality assurance step to ensure that the isolation method is not coisolating unwanted proteins, the PSC-derived EVs had slightly higher protein to lipid ratios than BMSCs. All groups fell within an acceptable range of a protein to lipid ratio <5, which was previously described by Osteikoetxea *et al.*[56] Another interesting result is that as the time of differentiation increased, the PSCs yielded lower lipid concentrations, whereas the lipid concentration increased for BMSCs. Taken together with the *in vitro* data, where dosages were based on protein concentrations, this implies that the PSC-derived EVs required a lower total number of EVs to achieve the same targeted differentiation effect as the BMSC-derived EVs.

The ability of PSC-derived EVs to be internalized by BMSCs was an important aspect of this study, suggesting that the EVs are not internalized by a cell-specific pathway. It was beyond the focus of this study to identify the individual surface proteins and glycoproteins expressed on each EV group or to determine the efficiency at which these EVs were internalized. Similarly, other groups commonly look at internalization qualitatively to determine whether or not the EVs are capable of internalization by the target cells.[33,57,58] But, by fluorescently labeling the EV membrane, it was observed that the EVs were internalized by cells *in vitro* regardless of cell source or differentiation time. Taken in combination with the results of the differentiation experiments, it can be assumed that EVs were internalized efficiently enough to achieve the targeted effect.

It was outside this study's scope to experimentally confirm the effect of each miRNA identified within our EVs. We observed a trend within both PSC and BMSC-derived EVs that resulted in the improved mineral deposition in 2D *in vitro* culture when delivering EVs from cells that were exposed to longer osteogenic differentiation times. This hints that the trend for miRNA profiles observed in BMSCs

between stages of differentiation is consistent within PSCs as well.[54] It is unclear whether these miRNAs are solely responsible for the osteogenic differentiation effect identified in the D21 group of EVs. It is much more likely that the effects observed are a result of a combination of bioactive molecules contained within the EVs, including these miRNAs. Regardless, we identified the relative expression levels of over 300 miRNAs and analyzed the differences in expression between cell source and stage of differentiation in an attempt to gain insight on whether these EVs are comparable in terms of miRNA profile.

Among the miRNAs differentially expressed between PSCs and BMSCs, miR-10b was dramatically increased in EVs from the D21 BMSC-derived EVs and was about 123 folds higher than PSCs (Supplementary Table S1). The TargetScan 7.2 software, which predicts biological targets of miRNAs based off of experimentally validated miRNA–gene interactions,[59] predicted that miR-10b can affect ID4 and indirectly promote osteoblast differentiation by enhancing RunX2 transcriptional activity.[60] Furthermore, it has been reported that miR-10b promotes the migration of MSCs into the bone microenvironment.[33,61]

It was also determined that the expression level of miR-21 increased twofold higher late-stage PSC and BMSC EVs in comparison to D0 EVs (Supplementary Table S1). The upregulation of miR-21 promotes osteogenesis through the PI3K/AKT/B-actin pathway and has effects on the mRNA expression, RUNX2, ALK, and OCN.[62] MiR-126-5p has also been found to regulate osteoclast differentiation and plays a role in bone remodeling through the inhibition of MMP-13.[63] Pathway analysis revealed the differentially expressed miRNA-targeted genes through multiple signaling pathways, such as *Wnt* signaling (Supplementary Fig. S1), MAPkinase, and TGFβ pathways (Supplementary Table S2). The varied, nonconsistent miRNA expressions between cell type and differentiation stage suggest a much more general trend toward osteogenesis, through many different pathways, as opposed to the expression of specific osteo-miRNAs that affect individual genes or pathways.

There were three miRNAs associated with increased osteogenesis that were expressed significantly higher in late-stage PSCs when compared with BMSCs. Most were associated with promoting osteoblast differentiation such as miR-146, miR-515, and miR-520a (Supplementary Table S3). The PSCs also significantly expressed two miRNAs, miR-512 and miR516b that were associated with inhibiting osteogenic differentiation and downregulating osteoblast differentiation, respectively.

There were various other osteo-related miRNAs that were downregulated at the later stages of differentiation such as miR-133, which is associated with the inhibition of osteoblast differentiation.[64] Although its expression decreased over time, it was still expressed ~twofold higher at late-stage PSC EV in comparison to BMSC EV. Other negative regulators of osteogenesis, such as let-7i, were found to be sixfold higher in BMSC EVs than PMSC EVs while still maintaining the trend of decreasing expression at later time points of differentiation. The importance of the expression levels of individual miRNAs remains unclear until further studies can identify their specific functions. When analyzing the trends of osteo-related miRNA, these miRNA expression levels are still consistent with the general trend toward increased osteogenesis in the late-stage EVs regardless of cell source. This was confirmed with *in vitro* uptake and differentiation experiments.

Based on our *in vitro* experiments, EVs derived from late-stage differentiation were able to achieve faster differentiation rates and improved mineral deposition when compared with our control. This is the result of delivering osteogenic miRNA as well as other potential osteogenic factors contained within the vesicles. Although the cell source had a large impact on the variety of miRNA contained within the EVs, the overall osteogenic impact was similar between the groups when comparing EVs derived at the same stage. All of the *in vitro* experiments chosen have been previously used to confirm osteogenic differentiation.[65] The improved bone mineral deposition resulting from delivering late-stage PSC and BMSC-derived EVs could potentially lead to the development of enhanced bone tissue engineering scaffolds or even improve fracture or nonunion healing.

All of these data taken together signify a new candidate from which to isolate osteogenic EVs. PSC's ease of donor availability, fast proliferation time, and high EV potency improve the likelihood that they will make a suitable candidate for clinical translation. The ability to easily scale up the isolation methods for these EVs, combined with their enhanced osteogenic differentiation rates, demonstrate their viability for future studies involving bone tissue engineering.

Conclusions

We compared PSC-derived EV's ability to differentiate cells *in vitro* with the well-characterized BMSC-derived EVs and proved the feasibility of utilizing these EVs for bone tissue engineering. We found that ALP activity and calcium deposition of BMSCs significantly increased when treated with late-stage-derived EVs, regardless of cell source. We have presented a comparative analysis of the miRNA content of these EVs, as well as identified potential pathways upon which these miRNAs are acting upon the cells. Since PSCs grow at a significantly faster rate than BMSCs, and also yield more potent EVs, they are a promising alternative source to utilizing BMSC-derived EVs for studies that require large amounts of EVs or need a high yield for therapeutic effects. During differentiation, EVs derived from late-stage osteogenic culture enhanced the rate of differentiation and mineralization of BMSCs regardless of stem cell source. This is a result of the uptake and delivery of the biologically active molecules contained within the EVs such as miRNAs. We hope that this information can lead to future studies improving the delivery mechanisms of EVs so they can overcome limitations with current bone grafting techniques by increasing native bone cell activity.

Acknowledgment

The authors would like to thank Mr. Kyung Whan Yoo for his technical support.

Disclosure Statement

No competing financial interests exist.

Funding Information

This study was supported by the National Science Foundation (NSF, Award #1663128) and the State of North Carolina. This work was supported, in part, by the Cancer

Genomics Shared Resource supported by the Wake Forest Baptist Comprehensive Cancer Center's NCI Cancer Center Support Grant P30CA012197-39.

Supplementary Material

Supplementary Figure S1
Supplementary Table S1
Supplementary Table S2
Supplementary Table S3

References

1. Amini, A.R., Laurencin, C.T., and Nukavarapu, S.P. Bone tissue engineering: recent advances and challenges. Crit Rev Biomed Eng **40,** 363, 2012.
2. Brooks, P.M. The burden of musculoskeletal disease—a global perspective. Clin Rheumatol **25,** 778, 2006.
3. O'Keefe, R.J., and Mao, J. Bone tissue engineering and regeneration: from discovery to the clinic—an overview. Tissue Eng Part B Rev **17,** 389, 2011.
4. Holland, T.A., and Mikos, A.G. Biodegradable polymeric scaffolds. Improvements in bone tissue engineering through controlled drug delivery. Adv Biochem Eng Biotechnol **102,** 161, 2006.
5. Marolt Presen, D., Traweger, A., Gimona, M., and Redl, H. Mesenchymal stromal cell-based bone regeneration therapies: from cell transplantation and tissue engineering to therapeutic secretomes and extracellular vesicles. Front Bioeng Biotechnol **7,** 352, 2019.
6. De Witte, T.-M., Fratila-Apachitei, L.E., Zadpoor, A.A., and Peppas, N.A. Bone tissue engineering via growth factor delivery: from scaffolds to complex matrices. Regen Biomater **5,** 197, 2018.
7. Vieira, S., Vial, S., Reis, R.L., and Oliveira, J.M. Nanoparticles for bone tissue engineering. Biotechnol Prog **33,** 590, 2017.
8. Bessa, P.C., Machado, R., Nürnberger, S., *et al.* Thermoresponsive self-assembled elastin-based nanoparticles for delivery of BMPs. J Control Release **142,** 312, 2010.
9. Cao, L., Wang, J., Hou, J., Xing, W., and Liu, C. Vascularization and bone regeneration in a critical sized defect using 2-N, 6-O-sulfated chitosan nanoparticles incorporating BMP-2. Biomaterials **35,** 684, 2014.
10. Li, L., Zhou, G., Wang, Y., Yang, G., Ding, S., and Zhou, S. Controlled dual delivery of BMP-2 and dexamethasone by nanoparticle-embedded electrospun nanofibers for the efficient repair of critical-sized rat calvarial defect. Biomaterials **37,** 218, 2015.
11. Zhang, S., Wang, G., Lin, X., *et al.* Polyethyleniminecoated albumin nanoparticles for BMP-2 delivery. Biotechnol Prog **24,** 945, 2008.
12. Wang, J., Liu, S., Li, J., Zhao, S., and Yi, Z. Roles for miRNAs in osteogenic differentiation of bone marrow mesenchymal stem cells. Stem Cell Res Ther **10,** 197, 2019.
13. Kim, N., Yoo, J.J., Atala, A., and Lee, S.J. Combination of small RNAs for skeletal muscle regeneration. FASEB J **30,** 1198, 2016.
14. Dong, S., Yang, B., Guo, H., and Kang, F. MicroRNAs regulate osteogenesis and chondrogenesis. Biochem Biophys Res Commun **418,** 587, 2012.
15. Li, Y., Fan, L., Liu, S., *et al.* The promotion of bone regeneration through positive regulation of angiogenic–osteogenic coupling using microRNA-26a. Biomaterials **34,** 5048, 2013.
16. Qin, Y., Wang, L., Gao, Z., Chen, G., and Zhang, C. Bone marrow stromal/stem cell-derived extracellular vesicles regulate osteoblast activity and differentiation in vitro and promote bone regeneration in vivo. Sci Rep **6,** 21961, 2016.
17. Jing, D., Hao, J., Shen, Y., *et al.* The role of microRNAs in bone remodeling. Int J Oral Sci **7,** 131, 2015.
18. Zhang, Y., Wang, Z., and Gemeinhart, R.A. Progress in microRNA delivery. J Control Release **172,** 962, 2013.
19. Radmanesh, F., Abandansari, H.S., Pahlavan, S., *et al.* Optimization of miRNA delivery by using a polymeric conjugate based on deoxycholic acid-modified polyethylenimine. Int J Pharm **565,** 391, 2019.
20. Shi, C., Qi, J., Huang, P., *et al.* MicroRNA-17/20a inhibits glucocorticoid-induced osteoclast differentiation and function through targeting RANKL expression in osteoblast cells. Bone **68,** 67, 2014.
21. Tang, X., Lin, J., Wang, G., and Lu, J. MicroRNA-433-3p promotes osteoblast differentiation through targeting DKK1 expression. PLoS One **12,** e0179860, 2017.
22. Garcia-Contreras, M., Shah, S.H., Tamayo, A., *et al.* Plasma-derived exosome characterization reveals a distinct microRNA signature in long duration Type 1 diabetes. Sci Rep **7,** 5998, 2017.
23. Li, W., Liu, Y., Zhang, P., *et al.* Tissue-engineered bone immobilized with human adipose stem cells-derived exosomes promotes bone regeneration. ACS Appl Mater Interfaces **10,** 5240, 2018.
24. Andaloussi, S.E.L., Lakhal, S., Mäger, I., and Wood, M.J.A. Exosomes for targeted siRNA delivery across biological barriers. Adv Drug Deliv Rev **65,** 391, 2013.
25. Behera, J., and Tyagi, N. Exosomes: mediators of bone diseases, protection, and therapeutics potential. Oncoscience **5,** 181, 2018.
26. Barlow, S., Brooke, G., Chatterjee, K., *et al.* Comparison of human placenta-and bone marrow–derived multipotent mesenchymal stem cells. Stem Cells Dev **17,** 1095, 2008.
27. Huang, L., Ying, H., Chen, Z., *et al.* Down-regulation of DKK1 and Wnt1/β-catenin pathway by increased homeobox B7 resulted in cell differentiation suppression of fetal intrauterine growth retardation in human placenta. Placenta **80,** 27, 2019.
28. Sung, H.J., Hong, S.C., Yoo, J.H., *et al.* Stemness evaluation of mesenchymal stem cells from placentas according to developmental stage: comparison to those from adult bone marrow. J Korean Med Sci **25,** 1418, 2010.
29. In't Anker, P.S., Scherjon, S.A., Kleijburg-van der Keur, C., *et al.* Isolation of mesenchymal stem cells of fetal or maternal origin from human placenta. Stem Cells **22,** 1338, 2004.
30. Zhang, Y., Li, C.-D., Jiang, X.-X., Li, H.-L., Tang, P.-H., and Mao, N. Comparison of mesenchymal stem cells from human placenta and bone marrow. Chin Med J (Engl) **117,** 882, 2004.
31. Youssef, A., and Han, V.K.M. Regulation of osteogenic differentiation of placental-derived mesenchymal stem cells by insulin-like growth factors and low oxygen tension. Stem Cells Int **2017,** 4576327, 2017.
32. Wolbank, S., Peterbauer, A., Fahrner, M., *et al.* Dose-dependent immunomodulatory effect of human stem cells from amniotic membrane: a comparison with human mesenchymal stem cells from adipose tissue. Tissue Eng **13,** 1173, 2007.
33. Wang, X., Omar, O., Vazirisani, F., Thomsen, P., and Ekström, K. Mesenchymal stem cell-derived exosomes have altered microRNA profiles and induce osteogenic differ-

entiation depending on the stage of differentiation. PLoS One **13,** e0193059, 2018.
34. Yoo, K.W., Li, N., Makani, V., Singh, R.N., Atala, A., and Lu, B. Large-scale preparation of extracellular vesicles enriched with specific microRNA. Tissue Eng Part C Methods **24,** 637, 2018.
35. Lee, M., Ban, J.-J., Im, W., and Kim, M. Influence of storage condition on exosome recovery. Biotechnol Bioprocess Eng **21,** 299, 2016.
36. Théry, C., Witwer, K.W., Aikawa, E., *et al.* Minimal information for studies of extracellular vesicles 2018 (MISEV2018): a position statement of the International Society for Extracellular Vesicles and update of the MISEV2014 guidelines. J Extracell Vesicles **7,** 1535750, 2018.
37. Vlachos, I.S., Zagganas, K., Paraskevopoulou, M.D., *et al.* DIANA-miRPath v3. 0: deciphering microRNA function with experimental support. Nucleic Acids Res **43,** W460, 2015.
38. Vlachos, I.S., and Hatzigeorgiou, A.G. Functional analysis of miRNAs using the DIANA Tools online suite. Methods Mil Biol **1517,** 25, 2017.
39. Maragkakis, M., Reczko, M., Simossis, V.A., *et al.* DIANA-microT web server: elucidating microRNA functions through target prediction. Nucleic Acids Res **37,** W273, 2009.
40. Paraskevopoulou, M.D., Georgakilas, G., Kostoulas, N., *et al.* DIANA-microT web server v5. 0: service integration into miRNA functional analysis workflows. Nucleic Acids Res **41,** W169, 2013.
41. Reczko, M., Maragkakis, M., Alexiou, P., Grosse, I., and Hatzigeorgiou, A.G. Functional microRNA targets in protein coding sequences. Bioinformatics **28,** 771, 2012.
42. Vlachos, I.S., Paraskevopoulou, M.D., Karagkouni, D., *et al.* DIANA-TarBase v7. 0: indexing more than half a million experimentally supported miRNA: mRNA interactions. Nucleic Acids Res **43,** D153, 2014.
43. Wang, X., Liao, X., Huang, K., *et al.* Clustered microRNAs hsa-miR-221-3p/hsa-miR-222-3p and their targeted genes might be prognostic predictors for hepatocellular carcinoma. J Cancer **10,** 2520, 2019.
44. Tang, Y.-T., Huang, Y.-Y., Zheng, L., *et al.* Comparison of isolation methods of exosomes and exosomal RNA from cell culture medium and serum. Int J Mol Med **40,** 834, 2017.
45. Zhang, J., Li, S., Li, L., *et al.* Exosome and exosomal microRNA: trafficking, sorting, and function. Genomics Proteomics Bioinformatics **13,** 17, 2015.
46. Kim, J.H., Liu, X., Wang, J., *et al.* Wnt signaling in bone formation and its therapeutic potential for bone diseases. Ther Adv Musculoskelet Dis **5,** 13, 2013.
47. Hao, Z.C., Lu, J., Wang, S.Z., Wu, H., Zhang, Y.T., and Xu, S.G. Stem cell-derived exosomes: a promising strategy for fracture healing. Cell Prolif **50,** e12359, 2017.
48. Fang, S., Li, Y., and Chen, P. Osteogenic effect of bone marrow mesenchymal stem cell-derived exosomes on steroid-induced osteonecrosis of the femoral head. Drug Des Devel Ther **13,** 45, 2019.
49. Liu, J., Li, D., Wu, X., Dang, L., Lu, A., and Zhang, G. Bone-derived exosomes. Curr Opin Pharmacol **34,** 64, 2017.
50. Liu, M., Sun, Y., and Zhang, Q. Emerging role of extracellular vesicles in bone remodeling. J Dent Res **97,** 859, 2018.
51. Qin, Y., Sun, R., Wu, C., Wang, L., and Zhang, C. Exosome: a novel approach to stimulate bone regeneration through regulation of osteogenesis and angiogenesis. Int J Mol Sci **17,** 712, 2016.
52. Qin, Y., Wang, L., Gao, Z., Chen, G., and Zhang, C. Bone marrow stromal/stem cell-derived extracellular vesicles regulate osteoblast activity and differentiation in vitro and promote bone regeneration in vivo. Sci Rep **6,** 1, 2016.
53. Cui, Y., Luan, J., Li, H., Zhou, X., and Han, J. Exosomes derived from mineralizing osteoblasts promote ST2 cell osteogenic differentiation by alteration of microRNA expression. FEBS Lett **590,** 185, 2016.
54. Gao, J., Yang, T., Han, J., *et al.* MicroRNA expression during osteogenic differentiation of human multipotent mesenchymal stromal cells from bone marrow. J Cell Biochem **112,** 1844, 2011.
55. Kalajzic, I., Matthews, B.G., Torreggiani, E., *et al.* In vitro and in vivo approaches to study osteocyte biology. Bone **54,** 296, 2013.
56. Osteikoetxea, X., Balogh, A., Szabó-Taylor, K., *et al.* Improved characterization of EV preparations based on protein to lipid ratio and lipid properties. PLoS One **10,** e0121184, 2015.
57. Bier, A., Berenstein, P., Kronfeld, N., *et al.* Placenta-derived mesenchymal stromal cells and their exosomes exert therapeutic effects in Duchenne muscular dystrophy. Biomaterials **174,** 67, 2018.
58. Mondal, A., Ashiq, K.A., Phulpagar, P., Singh, D.K., and Shiras, A. Effective visualization and easy tracking of extracellular vesicles in glioma cells. Biol Proced Online **21,** 4, 2019.
59. Karagkouni, D., Paraskevopoulou, M.D., Chatzopoulos, S., *et al.* DIANA-TarBase v8: a decade-long collection of experimentally supported miRNA–gene interactions. Nucleic Acids Res **46,** D239, 2018.
60. Tokuzawa, Y., Yagi, K., Yamashita, Y., *et al.* Id4, a new candidate gene for senile osteoporosis, acts as a molecular switch promoting osteoblast differentiation. PLoS Genet **6,** e1001019, 2010.
61. Weilner, S., Skalicky, S., Salzer, B., *et al.* Differentially circulating miRNAs after recent osteoporotic fractures can influence osteogenic differentiation. Bone **79,** 43, 2015.
62. Meng, Y.B., Li, X., Li, Z.Y., *et al.* microRNA-21 promotes osteogenic differentiation of mesenchymal stem cells by the PI3K/β-catenin pathway. J Orthop Res **33,** 957, 2015.
63. Wu, Z., Yin, H., Liu, T., *et al.* MiR-126-5p regulates osteoclast differentiation and bone resorption in giant cell tumor through inhibition of MMP-13. Biochem Biophys Res Commun **443,** 944, 2014.
64. Lv, H., Sun, Y., and Zhang, Y. MiR-133 is involved in estrogen deficiency-induced osteoporosis through modulating osteogenic differentiation of mesenchymal stem cells. Med Sci Monit **21,** 1527, 2015.
65. Jaiswal, N., Haynesworth, S.E., Caplan, A.I., and Bruder, S.P. Osteogenic differentiation of purified, culture-expanded human mesenchymal stem cells *in vitro*. J Cell Biochem **64,** 295, 1997.

Address correspondence to:
Sang Jin Lee, PhD
Wake Forest Institute for Regenerative Medicine
Wake Forest School of Medicine
Medical Center Boulevard
Winston-Salem, NC 27157
USA

E-mail: sjlee@wakehealth.edu

Received: July 10, 2020
Accepted: October 8, 2020
Online Publication Date: November 19, 2020